REPORT DOCU

AD-A236 810

READ INSTRUCTIONS BEFORE COMPLETING FORM

(2)

1. REPORT NUMBER
20

CIPIENT'S CATALOG NUMBER

4. TITLE (and Subtitle)
Discharge Poling and Poly(vinylidene fluoride) Films

PE OF REPORT & PERIOD COVERED
Technical

6. PERFORMING ORG. REPORT NUMBER

7. AUTHOR(s)
Y. Takase, J.I. Scheinbeim and B.A. Newman

8. CONTRACT OR GRANT NUMBER(s)
N00014-88-K-0122

9. PERFORMING ORGANIZATION NAME AND ADDRESS
Dept. of Mechanics and Materials Science
College of Engineering, Rutgers University
Piscataway, New Jersey 08855-0909

10. PROGRAM ELEMENT, PROJECT, TASK AREA & WORK UNIT NUMBERS

11. CONTROLLING OFFICE NAME AND ADDRESS
Dr. Joanne Milliken
Office of Naval Research
Arlington, VA 22217-5000

12. REPORT DATE
May 1991

13. NUMBER OF PAGES
25

14. MONITORING AGENCY NAME & ADDRESS(if different from Controlling Office)

15. SECURITY CLASS. (of this report)
UNCLASSIFIED

15a. DECLASSIFICATION/DOWNGRADING SCHEDULE

16. DISTRIBUTION STATEMENT (of this Report)
Approved for public release; distribution unlimited. Reproduction in whole or in part is permitted for any purpose of the United States Government.

17. DISTRIBUTION STATEMENT (of the abstract entered in Block 20, if different from Report)

18. SUPPLEMENTARY NOTES
Submitted, J. Appl. Phys.

19. KEY WORDS (Continue on reverse side if necessary and identify by block number)

20. ABSTRACT (Continue on reverse side if necessary and identify by block number)
A new poling technique was developed which is significantly different from the two conventional poling techniques; direct poling and corona poling. The present technique is based on the fact that the application of higher poling fields to poly(vinylidene fluoride) [PVF_2] films produces higher piezoelectric and pyroelectric responses but with a significantly higher risk of sample breakdown. This risk can be reduced by employing an active current limiter in the poling circuit. Experiments show that the risk of breakdown was significantly decreased

OVER

DD FORM 1 JAN 73 1473

91 6 12 046

UNCLASSIFIED
SECURITY CLASSIFICATION OF THIS PAGE (When Data Entered)

91-01967

by employing a discharge element connected in series with the sample. The element consits of a metal spark gap and a high resistance (1 GΩ) connected in series which works as a pulse shaper by suppressing the initial surge current and shutting down the current with a suitable time constant. PVF_2 films poled using the present method, under a voltage ramp up to 3000 V at 25°C exhibited significantly improved piezoelectric activity; piezoelectric strain and stress constants of 34 pC/N and 90 mC/m^2 (after 4 days aging) which are about 50% and 27% larger than normal values obtained by the direct poling method under 200 MV/m at 25°C.

OFFICE OF NAVAL RESEARCH

Contract N00014-88-K-0122

Technical Report No. 20

Discharge Poling and Poly(vinylidene fluoride) Films

by

Y. Takase, J.I. Scheinbeim and B.A. Newman

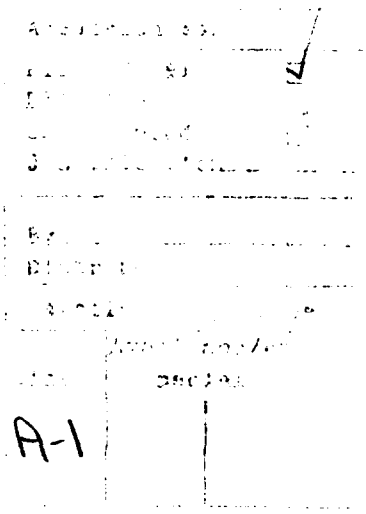

Prepared for Publication in

J. Appl. Phys.

Department of Mechanics and Materials Science
College of Engineering
Rutgers University
Piscataway, NJ 08855-0909

May 1991

Discharge poling of poly(vinylidene fluoride) films

Y. Takase, J. I. Scheinbeim, and B. A. Newman
Department of Mechanics and Materials Science, College of Engineering, Rutgers University, Piscataway, New Jersey 08854

A new poling technique was developed which is significantly different from the two conventional poling techniques; direct poling and corona poling. The present technique employs a negative-resistance switching circuit to allow the application of higher electric field to a sample without high risk of breakdown. The circuit consists of a high resistance, a spark gap, a sample to be poled and a small resistance connected in series. Shunted across the last three elements is a small capacitance. The circuit acts as a controlled pulse poling apparatus with the capability of feedback by detection of sample polarization. Poly(vinylidene fluoride) films (7 μm thick) poled using the present method, under a voltage ramp up to 3 kV at 25°C exhibited significantly improved piezoelectric activity; piezoelectric strain and stress constants of 34 pC/N and 90 mC/m^2 (after 4 days aging) which are about 48% and 27% larger than normal values obtained by the direct poling method under 200 MV/m at 25°C.

I. INTRODUCTION

It is well known that poly(vinylidene fluoride) [PVF_2] crystals with the phase I structure exhibit ferroelectricity and that PVF_2 films exhibit high piezoelectric activity after they are subjected to a poling procedure. To obtain the highest piezoelectric activity, it is of practical importance to find the optimum poling conditions. Poling is usually classified by using one of the following techniques; direct poling (or electrode poling) and corona poling. Direct poling is more suitable for basic research on these materials because the procedure is simple and allows for quantitative analysis. On the other hand, corona poling is more important for industrial uses such as poling of a large area of material or for some other special purpose in which the direct poling technique is difficult to apply.[1,2]

In both poling techniques, electric field, temperature and time are the most important parameters in the poling process. In the early stages of research on ferroelectric polymers, the poling temperature and time were set to be around 100°C and 1 h,[3-9] which was adapted from the traditional methods used for many inorganic ferroelectrics.[10,11] After accurate measurements of the time domain characteristics of the polarization switching process, however, it was recognized that it is not always necessary to keep the temperature as high as 100°C or to keep the time as long as 1 h. The switching of dipoles in PVF_2 is almost complete within the first 10 μs at room temperature, under an applied reversal electric field of 200 MV/m.[12,13] From these results, poling temperature and poling time are no longer considered important from an operational point of view. However, the

poling field strongly affects the resultant piezoelectric activity. Newman et al.,[14] Scheinbeim et al.[15] and Wang and von Seggern[16] investigated high field poling characteristics of PVF_2. Their data showed that the piezoelectric activity increased with increasing poling fields even at the maximum poling field range of 350 MV/m to 400 MV/m.

It seemed reasonable to assume that the risk of sample breakdown might be significantly reduced if a poling apparatus with capability of feedback by detection of sample polarization was employed.

In this paper, we present a new poling technique employing a negative-resistance switching circuit, which is quite different in behavior from the two conventional techniques, direct poling and corona poling, and which has some distinct merits with regard to yielding high piezoelectric activities when applied to PVF_2 films.

II. EXPERIMENTAL

Samples used in this study were 7-μm-thick uniaxially oriented PVF_2 films (KF1000) supplied by Kureha Chemical Industry, Co., Ltd. These films are the same as those used in several previous studies[12,13,17-19]. Annealed samples were prepared by heat treatment in vacuum at 120°C for 2 hours. During annealing, the films were mechanically clamped to prevent shrinkage.

Gold electrodes, each about 3 x 10 mm^2 in area, were deposited on opposing surfaces of the films by vacuum evaporation.

A block diagram of the poling arrangement is shown in

Fig. 1, where a source of high voltage V and a resistor R are connected to a pair of spark-gap electrodes, sample cell and a small resistor R_L (sum of input resistance of a current meter and resistances of a protection circuit). Shunted across the last three elements is a capacitor C, which may represent stray capacitance or capacitance deliberately introduced. The spark-gap electrodes used are either a pair of tungsten needles or a tungsten needle and a counter metal plate. The values of R and R_L are 0.5 - 2 GΩ and 10 kΩ - 1 MΩ, respectively, and the gap distance is 0.2 - 2 mm, depending on the sample to be poled. The sample cell is filled with silicone oil to prevent surface discharge along the fringe of the metal electrodes of the sample.

The current vs voltage characteristics of the poling arrangement and of the sample were measured at 25°C using a picoammeter (Keithley 485, input resistance is 100 kΩ). The period of the triangular shaped high voltage wave form was 640 s.

The time domain measurements of the discharge current were carried out using a digital signal recorder (Sony-Textronix 390 AD) which has a resolution of 10 bits and a maximum sampling frequency of 30 MHz.

The dielectric, elastic, and piezoelectric properties of the sample were measured by using a Rheolograph Solid® (Toyoseiki), which is capable of measuring dielectric constant, ϵ, Young's modulus, c, piezoelectric strain constant, d_{31}, and piezoelectric stress constant, e_{31}.

Operation of various functions in the system were consigned to a microcomputer which also performed the task of data processing.

III. RESULTS

The current vs voltage characteristics of the spark gap, which consists of a tungsten needle and a brass plate, are shown in Fig. 2. The values of R, C, R_L are 1 GΩ, 10 pF (stray capacitance) and 100 kΩ, respectively, and a triangular shaped voltage wave form with a maximum value of 3 kV was applied. The needle is connected to the high potential side. When the applied voltage exceeds a certain threshold value, a "noisy" current begins to flow. Although the current level fluctuates rapidly, there is a tendency for the average value of the current to increase as the voltage increases. Usually, it is observed that the threshold voltage on the negative side is smaller than that on the positive side. The temperature dependence of the current vs voltage characteristics was small and it was negligible between 0 to 60°C; the threshold voltage at -100°C became about twice as high as that at room temperature.

Figs. 3 (a) and (b) show the current vs voltage characteristics using the present poling procedure and of the direct poled PVF_2 film itself. The major characteristics of the combined element current vs voltage data are pulse-like current spikes concentrated around ±1.5 kV. The noise pulses are almost negligible in both regions of absolute voltage below 1 kV or above 2 kV. It may be reasonable to conclude from a comparison of the characteristics of the spark gap (Fig. 2) and the PVF_2 film that the pulses around ±1.5 kV originate from the combined phenomena of the spark gap and the polarization reversal process in the PVF_2

film.

The most striking result we observed after using the present poling technique is significantly higher values of piezoelectric constants for the poled PVF_2 films. Figs. 4 (a) and (b) show the real parts of the piezoelectric strain constant, d'_{31}, and piezoelectric stress constant, e'_{31}, as a function of applied electric field, E. Each value was measured 15 min after poling. Data (1) represent the result obtained from the as-stretched films by the present poling technique. The highest values of d'_{31} and e'_{31} are 48.5 pC/N and 108 mC/m^2, respectively. Data (2) (both curves) represent the results obtained for as-stretched films by the direct poling technique. Since the film used in the present study is highly oriented (draw ratio ≈5:1), the piezoelectric constants are large even if the conventional poling methods are used. However, under a high electric field of more than 200 MV/m, the risk of film breakdown increases significantly and the values of d'_{31} and e'_{31} never exceed 40 pC/N and 100 mC/m^2, respectively, during our experiments. Data (3) represent the result obtained for films annealed at 120°C. Piezoelectric activity always decreases for PVF_2 films annealed in the temperature region between 100 and 160°C before poling.[20]

Fig. 5 shows the aging characteristics of the real parts of the modulus, c', piezoelectric constants, d'_{31} and e'_{31}, and dielectric constant, ϵ', as a function of time after the sample was poled. Two different sets of data are presented, which represent data for the present discharge poling (circles) and for the direct poling (triangles). The maximum voltage applied was 3 kV for the discharge poling technique, and the maximum electric

field applied was 200 MV/m (voltage of about 1.4 kV) for the direct poling technique. During the direct poling procedure the risk of sample breakdown significantly increases even though the maximum voltage of the direct poling is about half of that of the discharge poling. Both poling process were carried out at 25°C. The data show that the sample poled with the discharge element exhibits values of d'_{31} and e'_{31} as high as 38.5 pC/N and 102.5 mC/m^2 (not the highest values shown in Fig. 4) 15 min after poling. These values are 126% and 121% of those obtained from a conventionally poled sample (d'_{31}=30.5 pC/N and e'_{31}=85.0 mC/m^2). After aging for about 4 days, the discharge-poled sample still shows higher values of d'_{31} and e'_{31}, 34 pC/N and 90 mC/m^2, respectively, which are 48% and 27% higher than those of a conventionally poled sample (d'_{31}=23 pC/N and e'_{31}=71 mC/m^2). The elastic modulus and the dielectric constant exhibit little difference between the two types of samples.

IV. DISCUSSION

It is well known that the spark gap exhibits a current-controllable negative resistance (NR) characteristic. First, we consider the basic circuit indicated in Fig. 6 (a),[21] where a source of voltage V and a resistor R are shown connected to an NR device and a small resistor R_L. The NR device has the current vs voltage (i vs v) characteristic of Fig. 6 (b). Shunted across the NR device and R_L is a capacitor C.

We are interested in the steady state corresponding to a particular value of supply voltage such as V_1, V_2 and V_3 shown in

Fig. 6 (b). The load lines are also plotted in Fig. 6 (b) as straight lines passing through the points $v = V_1$, V_2, V_3 and $i = 0$, and having a slope $-1/R$. When the current through the NR device is less than the threshold value (shown as point A in Fig. 6(b)) for a discharge phenomenon to occur, the operating point X_1 is a single stable point in the low-current region. When the supply voltage and load resistor are selected such that the load line intersects the characteristic at a single point X_2 on the NR portion of the characteristic (resistance $-R_n$), the circuit acts as a sawtooth waveform generator in an astable operation. This condition is expressed as $|-R_n| < R$ since the circuit response has the form of $\exp(-t/R_pC)$ with a positive exponent, where

$$R_p = -R_nR/(R - R_n) \qquad (1)$$

When the supply voltage is so high ($V = V_3$) that the operating point exceeds a negative resistance portion, the operating point X_3 becomes a single stable point in the high current region. The measured current-voltage characteristic of the spark gap, shown in Fig. 2, is essentially consistent with the characteristic predicted above in terms of the three operating conditions, single-stable-off, astable, and single-stable-on states.

In astable operation, the system will trace out the path B'AA'BB' in the direction of the arrows in Fig. 6(b). When the voltage exceeds the threshold voltage of the spark gap, the capacitance C discharges rapidly through the device and the small resistance R_L. The speed with which the voltage across R_L changes is determined by how quickly the device makes the transition from its low-current state to the state in which an avalanche dis-

charge is established. Having reached a peak, the output voltage across R_L now decays to zero as the capacitor discharges. The pulse width depends upon R_L and C and increases as the time constant R_LC increases. The rate at which the circuit may be driven is determined by R and C. Typically, for the present experiment, C ≈ 10 pF and R = 1 GΩ, whereas R_L = 100 kΩ, so that microsecond pulses with 10 millisecond spacing between pulses may be obtained.

Figure 7 shows results of the time domain measurements of the discharge pulse current. These characteristics were measured using the digital signal recorder. Curves (a) - (d) represent log J vs time characteristics obtained by using a resistor of R_L = 1 kΩ, 10 kΩ, 50 kΩ and 100 kΩ, respectively. Curve (e) represents a linear plot of curve (d). These characteristics show that the transition time from off to on state is quite short (nanosecond order) and the decay curve obeys an ideal single time constant relationship. The time constants are 0.05, 0.44, 2.3 and 4.5 μs for curves (a) - (d), respectively. These measured characteristics are just what we expected from the above discussion.

Now we can consider the circuit indicated in Fig. 1 which has a series combination of the spark gap and the PVF_2 sample. When the supply voltage is low, the spark gap and the sample are insulators. The voltage v_{gap} across the spark gap increases almost identically to the supply voltage V until its value reaches the threshold voltage of the discharge phenomenon, since

$$v_{gap} = V\, C_s/(C_{gap} + C_s), \qquad (2)$$

and, usually, the capacitance of the spark gap, C_{gap}, is much less than the capacitance of the sample C_s.

When the voltage is high enough to cause the discharge phenomenon to occur, the value of the resistance of the spark gap becomes negative. The value of the sample resistance R_s depends on the ferroelectric polarization reversal process and is complicated.[22] Under literally steady state conditions of an idealized capacitor, the value of R_s becomes infinity. The real device consists of the spark gap and the PVF_2 film. The discharge phenomenon is much faster (nanosecond order) than the ferroelectric polarization switching phenomenon (microsecond order or slower). Therefore, the sample may be regarded as a constant resistance during a discharge period. The characteristics of the combined device of spark gap and sample may be expressed by a series of quasi-steady-state current-voltage curves as shown in Fig. 8. The load lines are also plotted. The device characteristic continues to change from Curve 5 to Curve 1 and from Curve 1 to Curve 5 as the supply voltage increases. Curve 1 corresponds to the lowest sample resistance which may appear when the sample voltage reaches the coercive voltage. Under this condition, the device characteristic is almost the same as the spark gap. The combined device acts as a negative-resistance switch and the circuit operates as either an astable or a stable-on poling apparatus. When the operating point is far from the coercive field of the sample, the device characteristic exhibits little or no negative resistance portion. As a result, we observe significant current pulses only when the sample voltage passes the coercive voltage as the supply voltage increases. It is important to note that even under a

constant supply voltage, which gives a sample voltage higher than the coercive voltage, the device characteristics change from Curve 1 to Curve 5 as the polarization reversal completes. The operating point may move from X_1 to X_2, X_3, .., X_9 as shown schematically in Fig. 8 for a ramped and saturated supply voltage. The coercive voltage of the present 7-μm-thick sample is about 350 V which is much lower than the threshold voltage of the spark gap. Therefore, the measured current-voltage characteristic in Fig. 3 (a) may be interpreted in terms of this operating condition, though it may be necessary to note that the measured waveform is not accurate because the response of the picoammeter used was not fast enough to follow the microsecond-order phenomena. The change in the operating point represents a feedback process caused by sensing the sample polarization. The poling pulse height automatically decreases as the sample polarization reversal is completed, and, as a result, the circuit is quite effective in preventing sample breakdown.

The spark-gap distance may be chosen so that its threshold voltage exceeds the coercive voltage of the sample. The maximum value of the supply voltage may be twice (or more) as high as the value used in direct poling. Typically, for the present 7-μm-thick PVF_2 films, the risk of sample breakdown exceeded much more than 50% for direct poling under V = 1.75 kV or E = 250 MV/m, whereas it was rare in the present discharge poling under V = 3 kV. The time constants RC and R_LC can be adjusted so that the poling is effective without high risk of sample breakdown. Good results were obtained by choosing the value of RC much

larger than the value of R_LC which was adjusted close to the polarization switching time of the sample.

V. CONCLUSIONS

Piezoelectric constants d'_{31} and e'_{31} of poled PVF_2 films begin to increase at poling fields ≈ 80 MV/m, exhibit a shoulder around 150 MV/m and continue to increase as the poling field increases at room temperature. A negative-resistance switching circuit was constructed to apply the poling field. The apparatus was found to allow the application of higher electric fields to the sample without higher risk of breakdown. The circuit consisted of a high resistance (1 GΩ), a spark gap, a sample to be poled, and a small resistance (100 kΩ) connected in series. Shunted across the last three elements is a small capacitance (≈ 10 pF). The circuit acts as a controlled pulse poling apparatus with capability of feedback by detection of sample polarization. PVF_2 films poled by the present method at 25°C under a ramped electric field up to 3 kV showed significantly improved piezoelectric activities, d'_{31} = 34 pC/N and e'_{31} = 90 mC/m^2 after 4 days aging, which are compared to d'_{31} = 23 pC/N and e'_{31} = 71 mC/m^2 obtained by the conventional direct poling technique under a maximum electric field of 200 MV/m at 25°C.

ACKNOWLEDGMENT

The authors gratefully acknowledge the financial support of DARPA and the Office of Naval Research for these research studies.

[1]A. Ambrosy and K. Holdik, J. Phys. E: Sci. Instrum. **17**, 856 (1984).

[2]M. Imai, H. Tanizawa, Y. Ohtsuka, Y. Takase, and A. Odajima, J. Appl. Phys. **60**, 1916 (1986).

[3]H. Kawai, Jpn. J. Appl. Phys. **8**, 975 (1969).

[4]N. Murayama, J. Polymer Sci. Polym. Phys. Ed. **13**, 929 (1975).

[5]N. Murayama, T. Oikawa, T. Katto, and K. Nakamura, J. Polym. Sci. Polym. Phys. Ed. **13**, 1033 (1975).

[6]N. Murayama and H. Hashizume, J. Polym. Sci. Polym. Phys. Ed. **14**, 989 (1976).

[7]M. Oshiki and E. Fukada, Jpn. J. Appl. Phys. **15**, 43 (1976).

[8]R. G. Kepler and R. A. Anderson, J. Appl. Phys. **49**, 1232 (1978), **49**, 4490 (1978).

[9]T. Furukawa, J. Aiba, and E. Fukada, J. Appl. Phys. **50**, 3615 (1979).

[10]W. J. Merz, Rhys. Rev. **95**, 690 (1954).

[11]P. H. White and B. R. Withey, Brit. J. Appl. Phys. (J. Phys. D), **2**, 1487 (1969).

[12]T. Furukawa and G. E. Johnson, Appl. Phys. Lett. **38**, 1027 (1981).

[13]Y. Takase and A. Odajima, Jpn. J. Appl. Phys. **21**, L707 (1982).

[14]B. A. Newman, C. H. Yoon, K. D. Pae, and J. I. Scheinbeim, J. Appl. Phys. **50**, 6095 (1979).

[15]J. I. Scheinbeim and K. T. Chung, J. Appl. Phys. **52**, 5983 (1981).

[16]T. T. Wang and H. von Seggern, J. Appl. Phys. **54**, 4602 (1983).

[17]N. Takahashi and A. Odajima, Jpn. J. Appl. Phys. **20**, L59 (1981).

[18]T. Furukawa, M. Date, and G. E. Johnson, J. Appl. Phys. **54**, 1540 (1983).

[19]Y. Takase, A. Odajima, and T. T. Wang, J. Appl. Phys. **60**, 2920 (1986).

[20]Y. Takase, J. I. Scheinbeim, and B. A. Newman, J. Polym. Sci. Polym. Phys. Ed. **27**, 2347 (1989).

[21]J. Millman and H. Taub, Pulse, digital, and switching waveforms (McGraw-Hill, New York 1965), chapter 13.

[22]A. Fousková, J. Phys. Soc. Jpn. **20**, 1625 (1965).

Figure captions

FIG. 1. A block diagram of the poling arrangement, where a source of high voltage V and a resistor R are connected to a pair of spark-gap electrodes, sample cell and a small resistor R_L (sum of input resistance of a current meter and resistances of a protection circuit). Shunted across the last three elements is a capacitor C, which may represent stray capacitance or capacitance deliberately introduced.

FIG. 2. The current vs voltage characteristics of the spark gap, which consists of a tungsten needle and a brass plate. The values of R, C, R_L are 1 GΩ, 10 pF (stray capacitance) and 100 kΩ, respectively, and a triangular shaped voltage wave form with a maximum value of 3 kV was applied.

FIG. 3. (a) The current vs voltage characteristic during the present poling procedure. The values of R, C, R_L are 1 GΩ, 10 pF (stray capacitance) and 100 kΩ (input resistance of the picoammeter), respectively. (b) The current vs voltage characteristic of the PVF_2 film without the spark gap.

FIG. 4. The real parts of the piezoelectric strain constant, d'_{31}, and piezoelectric stress constant, e'_{31}, as a function of applied electric field. Each value was measured 15 min after poling. Data (1) represent the result obtained from the as-stretched films by the present poling technique. Data (2) (both curves) represent the results obtained for as-stretched films by the direct poling technique. Data (3) represent the result obtained for films annealed at 120°C.

FIG. 5. The aging characteristics of the real parts of the modulus, c', piezoelectric constants, d'_{31} and e'_{31}, and dielectric constant, ϵ', as a function of time after the sample was poled. Two different sets of data are presented, which represent data for the present discharge poling (circles) and for the direct poling (triangles).

FIG. 6. (a) A basic circuit where a source of voltage V and a resistor R are connected to a current-controllable negative-resistance (NR) device with the current-voltage characteristic of (b). Shunted across the NR device is a capacitor C. (b) The load lines corresponding to supply voltage $V = V_1$, V_2 and V_3, and resistance R are superimposed on the NR device characteristic.

FIG. 7. The time dependence of the discharge pulse current. Curves (a) - (d) represent log J vs time characteristics obtained by using a resistor R_L = 1 kΩ, 10 kΩ, 50 kΩ and 100 kΩ, respectively. Curve (e) represents a linear plot of curve (d).

FIG. 8. A schematic presentation of a series of quasi-steady-state current vs voltage curves which may represent characteristics of the combined device of the spark gap and the PVF_2 sample. The load lines corresponding to several supply voltages and resistance R are superimposed on the device characteristics. The calculation is based on a model that the characteristic of the spark gap is independent of load conditions, and the negative resistance and the on-state resistance are constant.

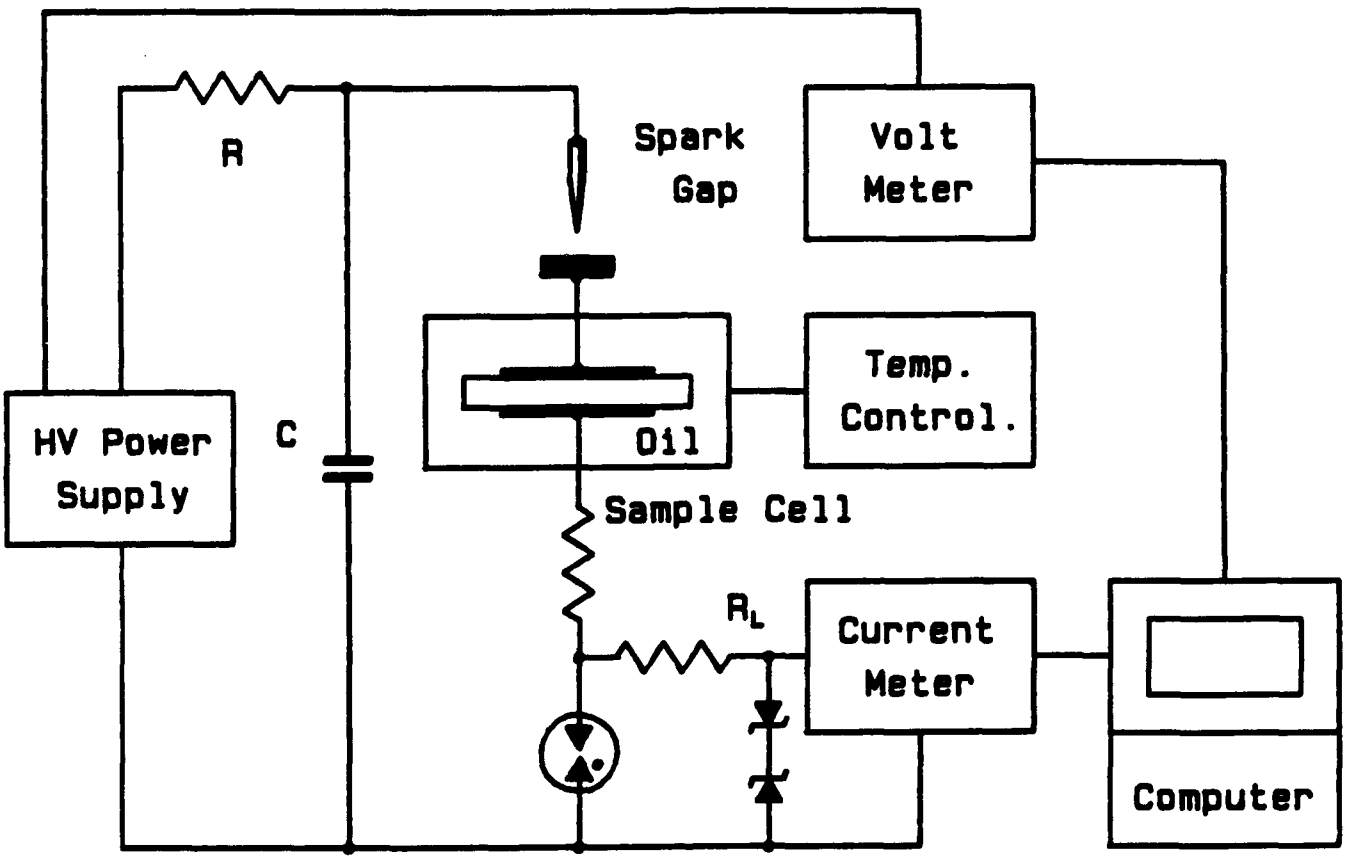
R
Spark
Gap
Volt
Meter
Temp.
Control.
HV Power
Supply
C
Oil
Sample Cell
R_L
Current
Meter
Computer

FIG. 1.

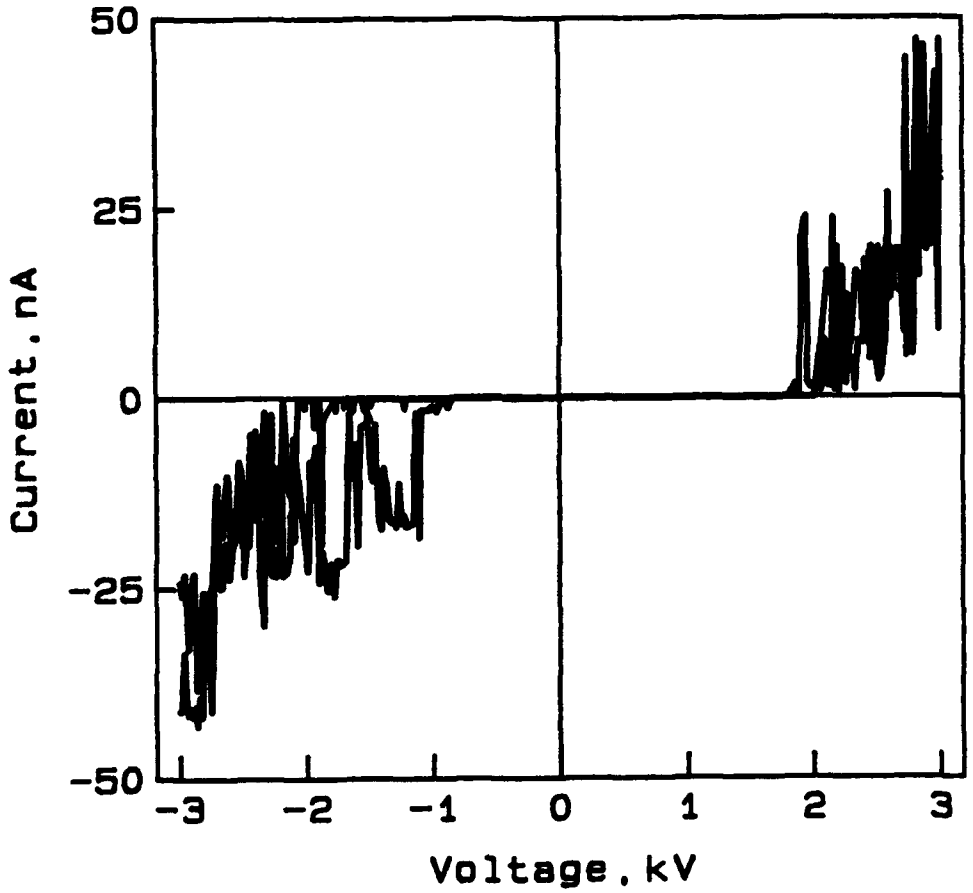

FIG. 2.

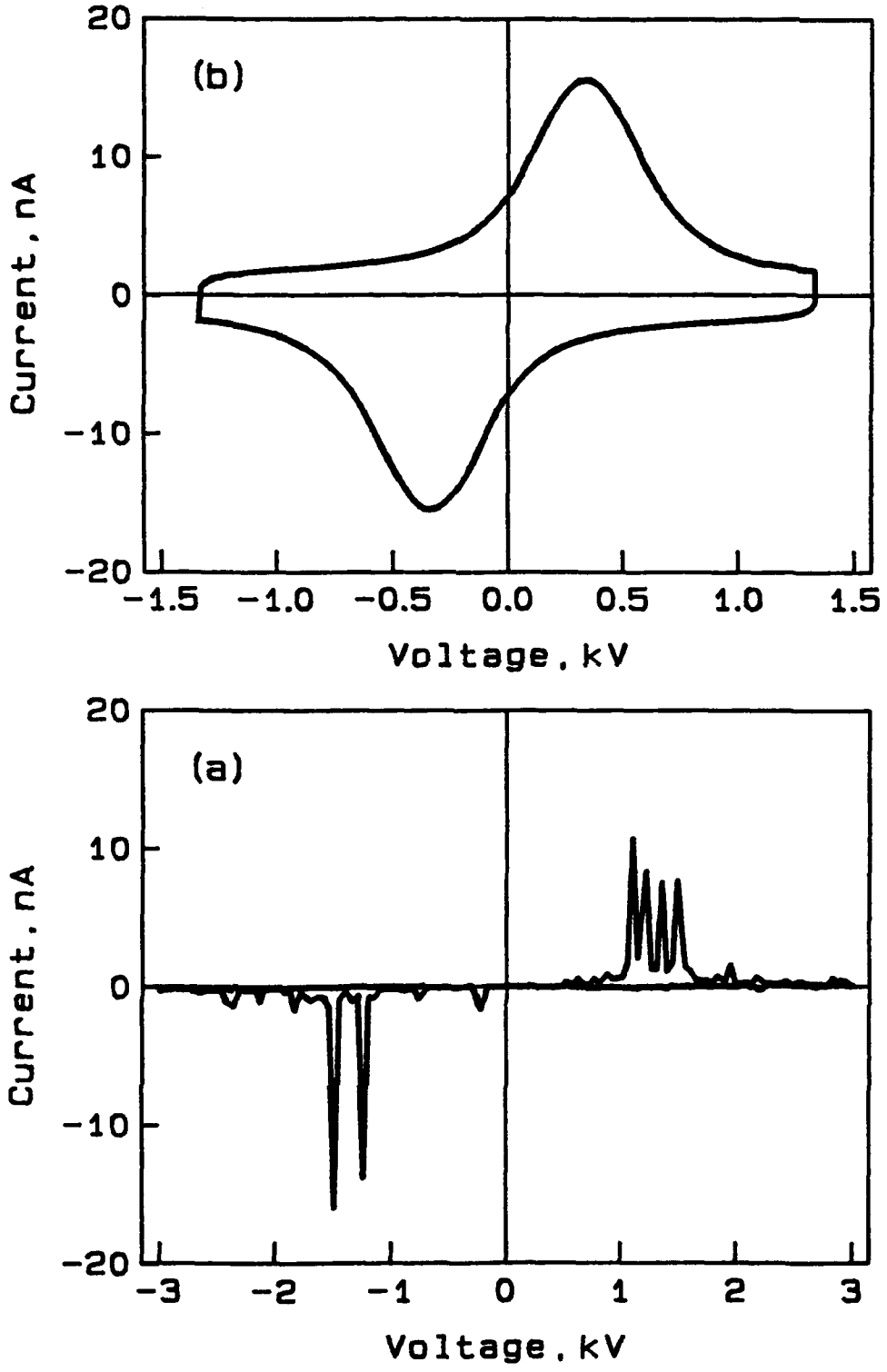
(b)
20
10
0
-10
-20
Current, nA
-1.5
-1.0
-0.5
0.0
0.5
1.0
1.5
Voltage, kV
(a)
20
10
0
-10
-20
Current, nA
-3
-2
-1
0
1
2
3
Voltage, kV

FIG. 3.

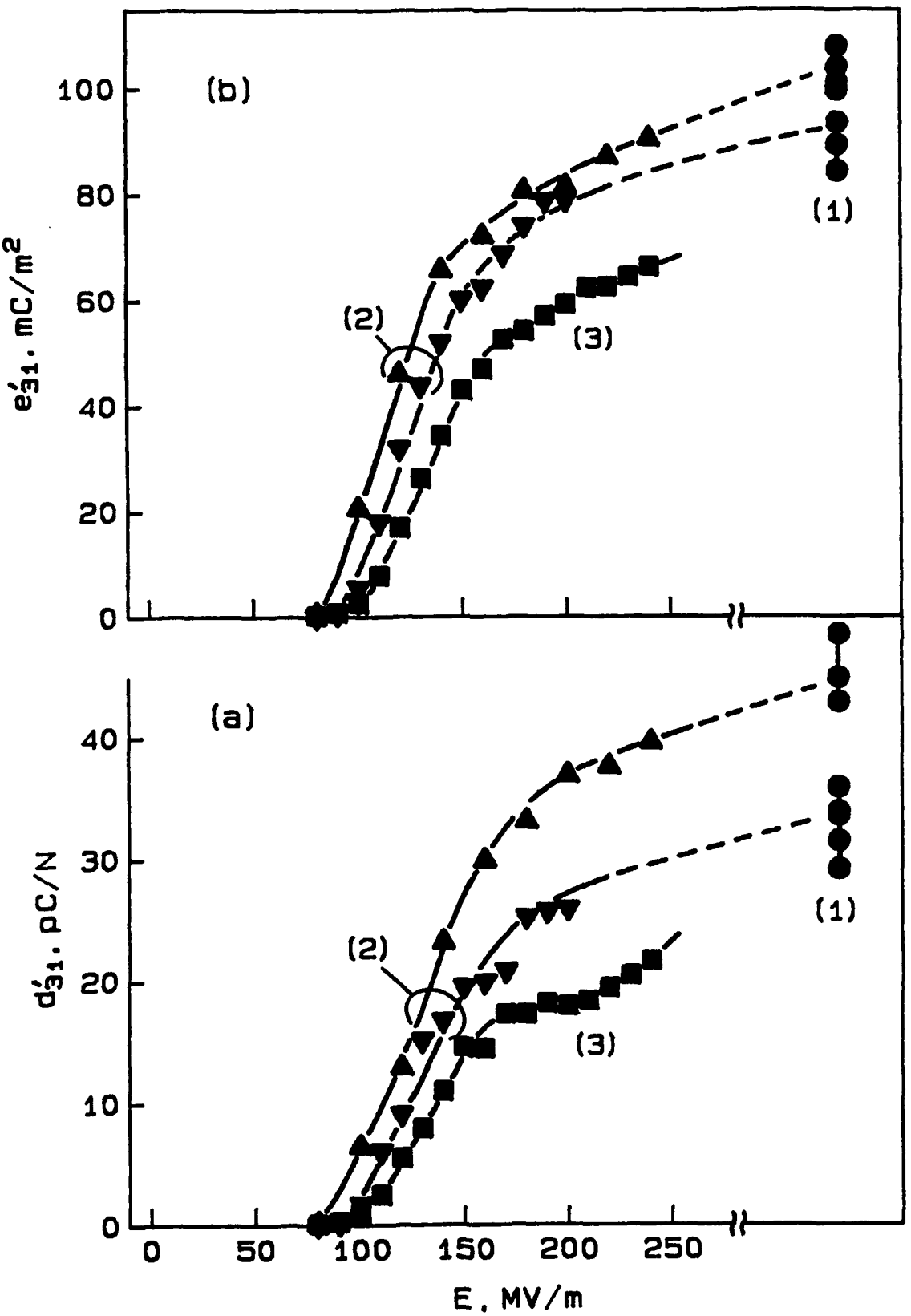
(b)
100
80
60
40
20
0
e'_{31}, mC/m^2
(1)
(2)
(3)
(a)
40
30
20
10
0
d'_{31}, pC/N
(1)
(2)
(3)
0
50
100
150
200
250
E, MV/m

FIG. 4.

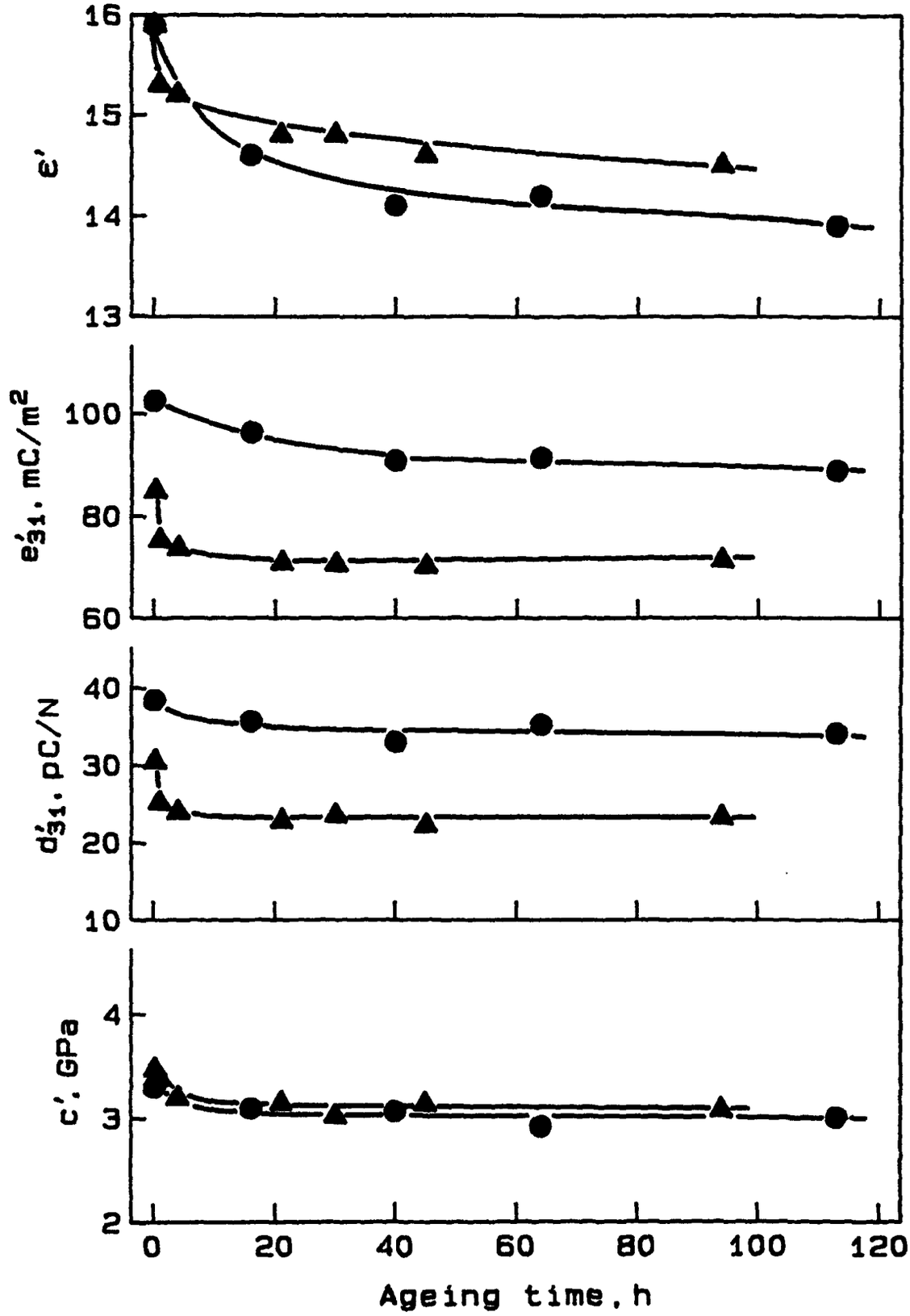
ε'
16
15
14
13
e'_{31}, mC/m²
100
80
60
d'_{31}, pC/N
40
30
20
10
c', GPa
4
3
2
0
20
40
60
80
100
120
Ageing time, h

FIG. 5.

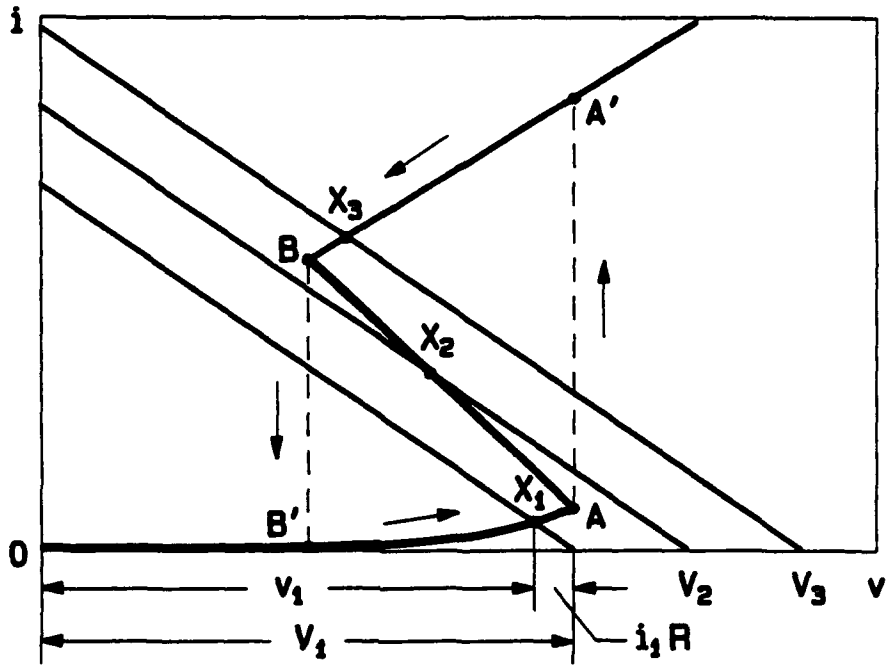

(b)

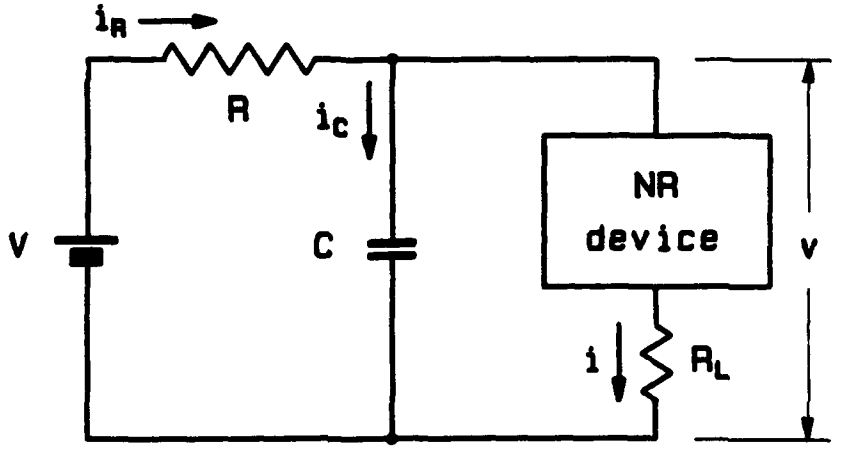

(a)

FLG. 6.

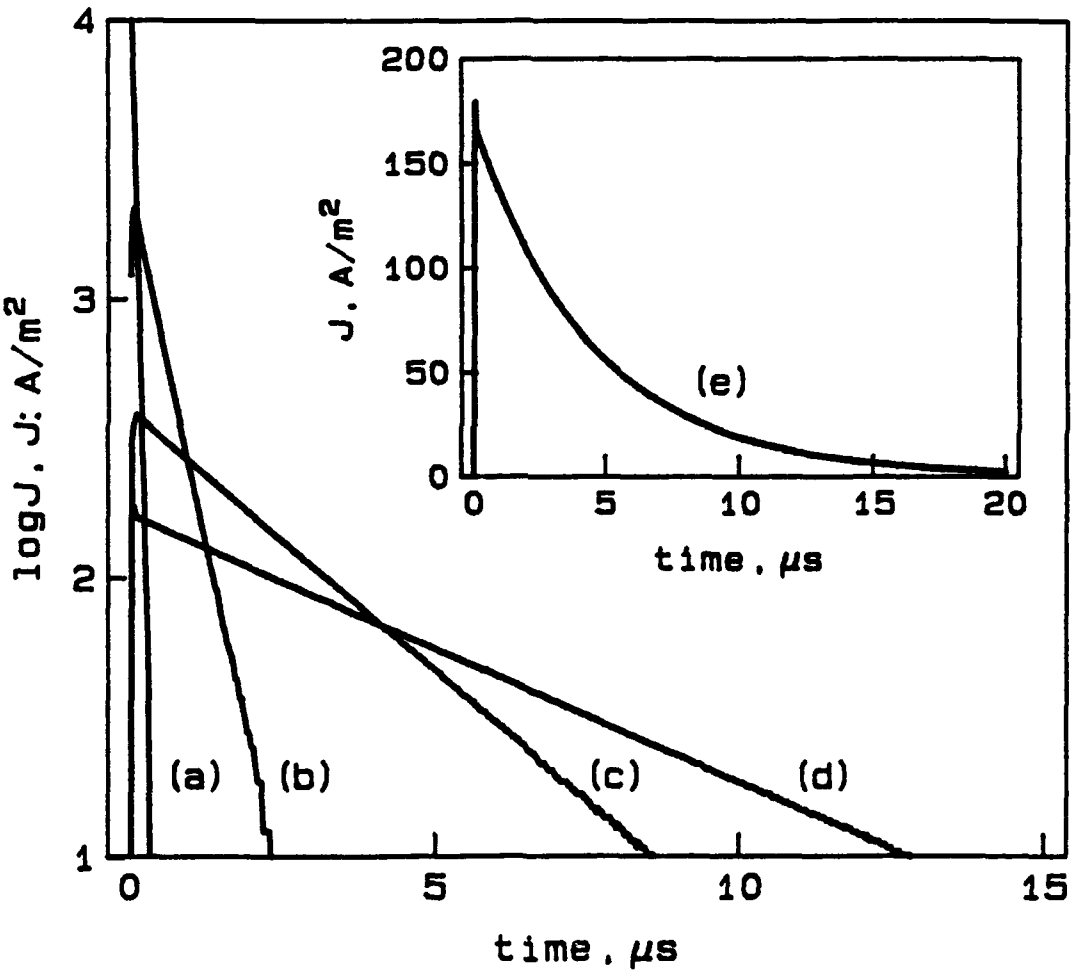
4
3
2
1
0
5
10
15
logJ, J: A/m²
time, μs
(a)
(b)
(c)
(d)
200
150
100
50
0
0
5
10
15
20
J, A/m²
time, μs
(e)

FIG. 7.

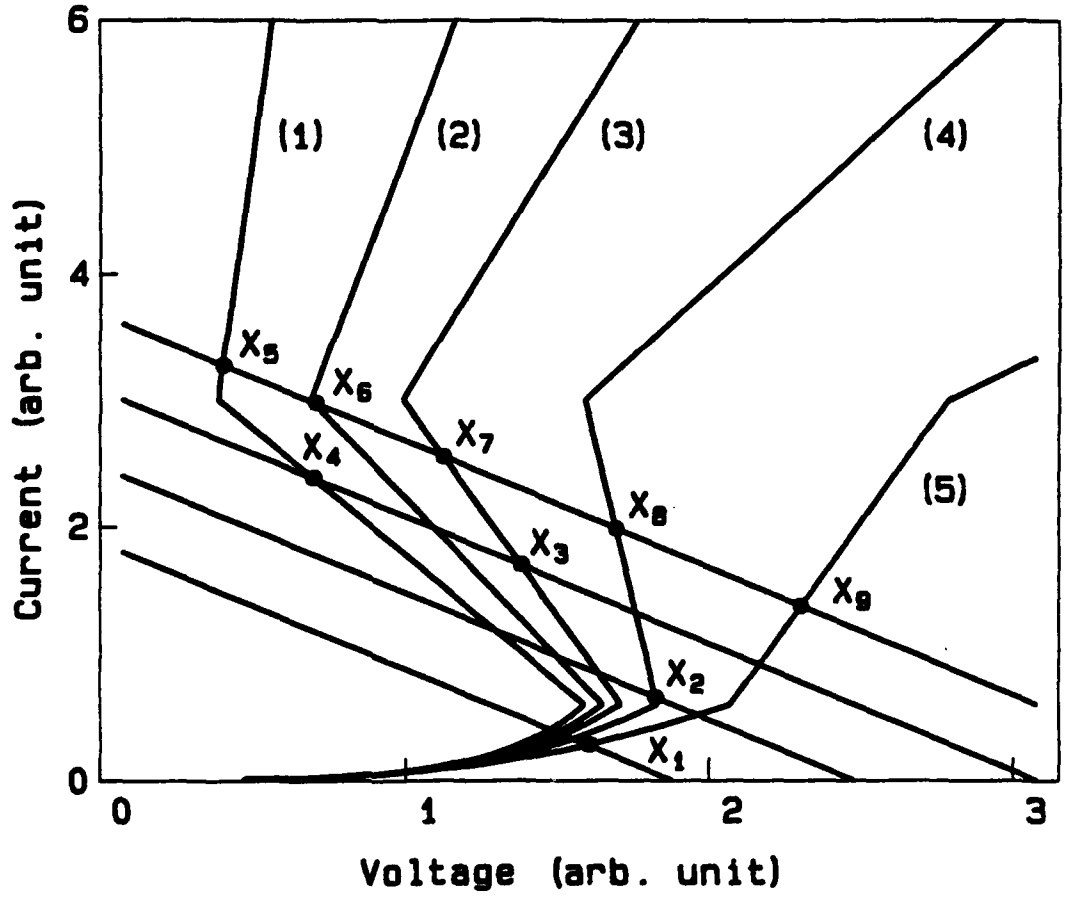
6
4
2
0
0
1
2
3
Current (arb. unit)
Voltage (arb. unit)
(1)
(2)
(3)
(4)
(5)
X1
X2
X3
X4
X5
X6
X7
X8
X9

FIG. 8.